Journal Pre-proof

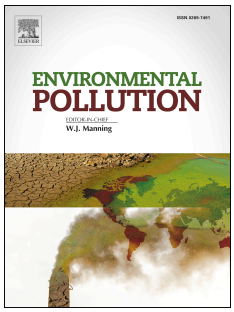

Environmental drivers of nitrous oxide emission factor for a coastal reservoir and its catchment areas in southeastern China

Ping Yang, Liangjuan Luo, Kam W. Tang, Derrick Y.F. Lai, Chuan Tong, Yan Hong, Linhai Zhang

PII: S0269-7491(21)02150-3

DOI: https://doi.org/10.1016/j.envpol.2021.118568

Reference: ENPO 118568

To appear in: *Environmental Pollution*

Received Date: 14 September 2021

Revised Date: 19 November 2021

Accepted Date: 20 November 2021

Please cite this article as: Yang, P., Luo, L., Tang, K.W., Lai, D.Y.F., Tong, C., Hong, Y., Zhang, L., Environmental drivers of nitrous oxide emission factor for a coastal reservoir and its catchment areas in southeastern China, *Environmental Pollution* (2021), doi: https://doi.org/10.1016/j.envpol.2021.118568.

Environmental drivers of nitrous oxide emission factor for a coastal reservoir and its catchment areas in southeastern China

Ping Yang[a,b*], Liangjuan Luo[a,b], Kam W. Tang[c], Derrick Y. F. Lai[d], Chuan Tong[a,b], Yan Hong[a], Linhai Zhang[a,b]

[a]*School of Geographical Sciences, Fujian Normal University, Fuzhou 350007, P.R. China*

[b]*Key Laboratory of Humid Subtropical Eco-geographical Process of Ministry of Education, Fujian Normal University, Fuzhou 350007, P.R. China*

[c]*Department of Biosciences, Swansea University, Swansea SA2 8PP, U. K.*

[d]*Department of Geography and Resource Management, The Chinese University of Hong Kong, Hong Kong, China*

***Correspondence to:**

yangping528@sina.cn (Ping Yang)

ABSTRACT

Asia is projected to be a major contributor to nitrous oxide (N_2O) emission in the coming decades, but assessment of N_2O budget and distribution has been hampered by low data resolution and poorly constrained emission factor (EF). Urbanized coastal reservoirs receive high nitrogen loads from diverse sources across a heterogeneous landscape, and using a fixed EF may lead to large errors in N_2O assessment. We conducted high spatial resolution sampling of dissolved N_2O, nitrate-nitrogen (NO_3^-–N) and related hydrographical parameters in Wenwusha Reservoir and its catchment areas (river, drainage channels, and aquaculture ponds) in southeastern China in November 2018, March 2019 and June 2019. The empirically derived EF (calculated as N_2O-N:NO_3^--N) for the reservoir showed 10-fold spatial variations, ranging from 0.8×10^{-3} to 8.8×10^{-3}. The average EF varied significantly among the four water types in the following descending order: aquaculture ponds > river > drainage channels > reservoir. Across all water types, EF of the summer month was 1.8–3.5 and 1.7–2.8 fold higher on average than that of autumn and spring, respectively. EF was higher in the summer likely due to elevated water temperature. Overall, the EF deviated considerably from the Intergovernmental Panel on Climate Change (IPCC) default value such that using the latter would result in over- or under-estimation of N_2O emissions, sometimes by up to 42%. A new regression algorithm for EF based on water temperature, dissolved organic carbon and nitrate-nitrogen had a high and significant explanatory power (r^2 = 0.82; p < 0.001), representing an improvement

over the IPCC default EF for assessing N_2O emission from coastal reservoirs and similar environments.

Keywords: N_2O; Greenhouse gas; IPCC; Spatio-temporal variation; Nitrate-nitrogen; Inland waters

1. Introduction

As a greenhouse gas, nitrous oxide (N_2O) has approximately 270 times the warming effect of carbon dioxide on a century timescale (Neubauer and Megonigal, 2015). The concentration of N_2O in the atmosphere increased at a rate of 0.7–0.8 ppbv per year in the past five decades (Davidson, 2009; Saikawa et al., 2014), and reached 334 ppbv in 2021 (National Oceanic and Atmospheric, 2021). Biological conversion of anthropogenic nitrogen to N_2O in soil and surface waters is estimated to contribute approximately 55% of the N_2O emission globally (Ciais et al., 2014; Zhang et al., 2020). Therefore, effective climate change mitigation will require better understanding of spatiotemporal distribution of N_2O emission and its environmental drivers.

N_2O emission from soil has been studied extensively (e.g., Griffis et al., 2013; Mosier et al.,1998) and is a relatively well-constrained component of the global N_2O assessment (Quick et al., 2019; Zhang et al., 2020). Agriculture accounts for the largest N_2O emission from soil (Tian et al., 2020). By comparison, N_2O emission from aquatic systems including those influenced by nutrient runoff is poorly constrained (Outram and Hiscock, 2012; Webb et al., 2021) and it remains a major source of uncertainty in the global N_2O budget.

Because of the chemical stability of N_2O in surface waters, N_2O emission is directly proportional to dissolved N_2O concentration. The production of N_2O itself, however, is a rather complex biogeochemical process as it can involve multiple precursors and redox reactions (Schreiber et al., 2012). In practice, the

Intergovernmental Panel on Climate Change (IPCC) estimates waterborne N_2O emission as anthropogenic N loading multiplied by an emission factor (EF) and leaching loss (IPCC, 2006). This approach is only suitable where the source and amount of N input from the catchment can be readily defined and leaching loss is known and invariant, such may be the case of fertilized farmland. Also, to initially establish the EF one needs N_2O emission that is usually estimated from dissolved N_2O concentration based on a wind-based gas transfer model, which itself is often not calibrated for the local conditions such as river flowrate and sheltering effect from the surrounding landscape (e.g., Qin et al. 2019). As such, application of the EF to running water through a variable landscape can lead to significant errors.

For urbanized and artificial aquatic systems such as coastal reservoirs, N_2O dynamics is compounded by N input from diverse and diffuse sources, such as contributions from wastewater discharge, fertilization (such as fish feeds in aquaculture ponds), leaching and runoff from surrounding landscape as well as atmospheric deposition, in addition to in situ N_2O production. To assess N_2O emission from such systems, an alternative EF can be calculated as the ratio between dissolved concentrations of nitrous oxide nitrogen (N_2O-N) and nitrate-nitrogen (NO_3^--N) (Hama-Aziz et al., 2017). This formulation is appealing because it uses parameters that can be measured easily and accurately, without prior knowledge of the source of N. Once the EF is established, it can be used to estimate N_2O-N from NO_3^--N, the latter of which is a routine parameter in environmental surveys, thereby facilitating the

85 spatiotemporal assessment of N_2O. However, the conversion of nitrogenous input or
86 NO_3^--N to N_2O is mediated by a multitude of biological and physical factors (Schreiber
87 et al., 2012) and therefore, applying a fixed EF could be problematic (Cooper et al.,
88 2017; Fu et al. 2018; Turner et al., 2015). Indeed, some researchers have argued that the
89 IPCC default EF may have grossly overestimated N_2O emission from inland waters
90 (Maavara et al., 2019).

91 Asia is projected to account for the largest share of riverine and estuarine N_2O
92 emission in the coming decades under various Millennium Ecosystem Assessment
93 scenarios (Kroeze et al., 2010). As population size increases in many Asian coastal
94 cities, construction of coastal reservoirs is widely considered as the solution to water
95 scarcity (Yang et al., 2018). Due to increasing agricultural activities and rapid
96 urbanization in the catchment areas, coastal reservoirs often receive high N loading
97 from multiple sources, making them potential N_2O hotspots (Lacerda et al., 2008;
98 Páez-Osuna et al., 2017). The high heterogeneity in geography and hydrography around
99 and within coastal reservoirs may require a more nuanced approach to derive EF in
100 order to improve the assessment of N_2O emission from these inland water systems.

101 We conducted a field study, using high spatial resolution data of dissolved N_2O
102 and NO_3^--N, to assess the variability of EF across a coastal reservoir and its catchment
103 areas (river, drainage channels and aquaculture ponds) in southeastern China. We also
104 examined the relationships between EF and different hydrographical parameters, based
105 on which we derived algorithms to improve EF value for N_2O emission assessment.

2. Materials and methods

2.1. Study area

The Wenwusha Reservoir is at the mouth of the Min River Estuary in southeastern China (25°49′36″ to 25°54′00″N, 119°35′12″ to 119°38′11″E), within a densely populated area with approximately1000 persons per km^2 (Fig. 1). The reservoir was constructed primarily for irrigation and flood mitigation purposes, and it covers 5.2 km^2 in surface area and 3.20 × 10^8 m^3 in volume. The reservoir receives input from a catchment area of 275 km^2 of diverse landscape features that include urban area (6.0%), aquaculture ponds (9.8%), forest (15.0%), farmland (3.3%), sand (2.1%) and wetland (14.4%) (Zhang et al., 2021). The reservoir is divided by dams into two basins (Fig. 1): the north basin (NB) is heavily impacted by domestic, industrial and aquacultural waste discharges as well as input from the Nanyangdong River; the south basin (SB) is surrounded by farmlands (including aquaculture), wetland, forest and towns. The region experiences subtropical monsoonal climate with an annual average temperature of 19.6 °C and precipitation of 1,390 mm (Yang et al., 2020).

2.2. Sample collection and analysis

High-resolution field sampling was conducted in November 2018 (autumn), March 2019 (spring) and June 2019 (summer), where a total of 121 sites were sampled each time, of which 103 sites were within the reservoir, seven in the river, four in

drainage channels, and seven in aquaculture ponds (Fig. 1). A total of 21 transects were sampled within the reservoir, with 11 transects in the south basin and 10 in the north basin (Fig. 1b).

To measure dissolved N_2O, water was collected from 20 cm below the surface with a syringe and transferred into 55-mL glass serum bottles. Microbial activities in the water sample were stopped by adding 0.2 mL saturated $HgCl_2$ solution (Zhang et al., 2013); the bottle was then sealed immediately without headspace with a butyl rubber stopper (Xiao et al., 2019a). Upon return to the laboratory, dissolved N_2O was measured using the headspace equilibration technique (Davidson et al., 2015; Yu et al., 2013). A headspace was created by displacing 25 mL of the water with nitrogen (N_2) (>99.999% purity). The bottle was then shaken for 10 minutes to attain gas equilibrium between the headspace and the liquid phase. 5 mL of the headspace gas was extracted and injected into a gas chromatograph (GC-2014, Shimadzu, Kyoto, Japan) equipped with an electron capture detector (ECD) for determining the N_2O concentration. A calibration curve was produced with standard N_2O gas at 0.3, 0.4 and 1.0 ppm. The N_2O measurements had a precision of ± 5% and a detection limit of 0.02 ppm.

Using the measured headspace N_2O concentrations, the original dissolved concentrations of dissolved N_2O were calculated based on the Bunsen solubility coefficient as a function of temperature and salinity (Brase et al., 2017; Weiss and Price, 1980). The N_2O emission factor (EF) was calculated as the ratio between N_2O-N and NO_3^--N dissolved concentrations (Hama-Aziz et al., 2017) for the surface waters of the

147 reservoir, river, drainage channels and aquaculture ponds.

148 Additional water samples were collected into 150 mL polyethylene bottles at each
149 site and filtered through a 0.45 μm cellulose acetate filter (Biotrans™ nylon
150 membranes). The filtrates were analyzed for nitrate-nitrogen (NO_3^--N) and total
151 dissolved nitrogen (TDN) by a flow injection analyzer (Skalar Analytical SAN^{++},
152 Netherlands), and dissolved organic carbon (DOC) by a TOC analyzer
153 (TOC-VCPH/CPN, Shimadzu, Japan). The detection limit and relative standard
154 deviations were 0.6 μg L^{-1} and ⩽ 2.0% for NO_3^--N, 3.0 μg L^{-1} and ⩽ 2.0% for TDN,
155 and 0.4 μg L^{-1} and ⩽ 1.0% for TOC, respectively.

156 In each sampling campaign, we also measured various hydrographical parameters
157 of surface water in situ at a depth of 20 cm at each site. Water temperature (T_W) and pH
158 were measured by a portable meter (IQ150, IQ Scientific Instruments, USA).
159 Conductivity (EC), dissolved oxygen (DO) and chemical oxygen demand (COD) were
160 determined by a EC meter (2265FS EC, Spectrum Technologies, USA), a water quality
161 checker (HORIBA, Japan) and a COD detector (LH-CM3H, China), respectively.

162 *2.3. Statistical analysis*

163 Statistical tests were conducted in SPSS version 17.0 (SPSS Inc., USA) at a
164 significance level of $p < 0.05$. Differences in hydrographical properties, dissolved N_2O
165 concentration and EF between water bodies (e.g., reservoir, river, drainage channels,
166 aquaculture ponds) and between reservoir basins (e.g., north basin and south basin)
167 were tested by one-way analysis of variance (ANOVA). Relationships between

hydrographical parameters and EF were tested by Pearson correlation analysis. OriginPro version 7.5 (OriginLab Corp. USA) was used to generate the statistical plots. The Kriging method in ArcGIS 10.2 (ESRI Inc., Redlands, CA, USA) was used for spatial interpolation of EF in the reservoir. All results were presented as mean ± 1 standard error (S.E.), unless otherwise stated.

3. Results

3.1. Hydrographical conditions

There was no significant difference in mean surface water T_W among the four water types ($p > 0.05$; Fig. 2a). However, the surface water chemical properties varied greatly. Overall, the mean pH (Fig. 2b) and EC (Fig. 2c) were highest in aquaculture ponds (9.5 ± 0.6 and 3.49 ± 1.79 mS cm^{-1}, respectively), followed by reservoir (8.7 ± 1.1 and 2.6 ± 1.0 mS cm^{-1}), drainage channels (8.1 ± 0.3 and 1.8 ± 0.5 mS cm^{-1}) and river (7.7 ± 0.2 and 1.3 ± 0.3 mS cm^{-1}) ($p < 0.05$). The mean DOC concentration was also highest in aquaculture ponds (8.4 ± 2.3 mg L^{-1}), followed by river (7.4 ± 2.0 mg L^{-1}), drainage channels (7.2 ± 1.8 mg L^{-1}) and reservoir (4.1 ± 0.9 mg L^{-1}) (Fig. 2f). In the river, the mean DO (4.0 ± 0.3 mg L^{-1}) (Fig. 2d) and COD (23.3 ± 2.4 mg L^{-1}) (Fig. 2e) concentrations were significantly lower ($p < 0.05$) while NO_3^--N (1.64 ± 0.2 mg L^{-1}) (Fig. 2g) and TDN (2.2 ± 0.4 mg L^{-1}) (Fig. 2h) concentrations were generally higher than in the other areas ($p < 0.05$).

The hydrographical conditions also showed strong temporal variations. Across the

four surface water types, the mean T_W (28.1 ± 0.5 ^oC) (Fig. 2a) and DOC (9.9 ± 1.4 mg L^{-1}) (Fig. 2f) were highest in summer, whereas the mean pH (9.5 ± 0.7) (Fig. 2b) and EC (3.8 ± 1.2 mS cm^{-1}) (Fig. 2c) were highest in autumn. We observed generally higher DO (7.4 ± 1.2 mg L^{-1}) (Fig. 2d) in spring and higher COD (34.5 ± 3.0 mg L^{-1}) (Fig. 2e) in autumn. The mean NO_3^--N (Fig. 2g) and TDN (Fig. 2h) concentrations in river (2.0 ± 0.3 mg L^{-1} and 2.9 ± 0.1 mg L^{-1}, respectively) and drainage channels (1.4 ± 0.1 and 2.5 ± 0.1 mg L^{-1}) were highest in spring; in contrast, the mean NO_3^--N (Fig. 2g) and TDN (Fig. 2h) concentrations in aquaculture ponds (1.4 ± 0.1 and 1.4 ± 0.1 mg L^{-1}) and reservoir (2.2 ± 0.1 and 1.9 ± 0.1 mg L^{-1}) were highest in autumn.

3.2. N_2O concentration in surface waters

The dissolved N_2O concentration in river, drainage channels and aquaculture ponds varied seasonally in this decreasing order: summer > spring > autumn (Fig. 3). In the reservoir, the mean N_2O concentration was slightly higher in spring (Fig. 3). Across all sampling dates and sites, the N_2O concentration in river, drainage channels, aquaculture ponds, and reservoir varied over the range of 49.6–261.3, 42.8–121.8, 42.2–198.9, and 6.1–261.2 nmol L^{-1}, respectively. Over the study period, there was a significant difference in N_2O concentration between surface water types ($p < 0.001$; Table 1), with the highest value in river (110.0 ± 36.1 nmol L^{-1}), followed by aquaculture ponds (91.7 ± 29.2 nmol L^{-1}), drainage channels (75.9 ± 8.2 nmol L^{-1}) and reservoir (49.8 ± 4.6 nmol L^{-1}).

3.3. Spatial and seasonal variations of EF

Across the reservoir, there were clear spatial differences in EF between the two basins (ANOVA, $p < 0.05$; Fig. 4). Overall, EF in NB ranged from 0.3×10^{-3} to 8.8×10^{-3}, which were higher than that in SB (0.4×10^{-3}–6.6×10^{-3}) (Fig. 4d). Significant differences were also observed between sampling sites with respect to wastewater discharge (ANOVA, $p < 0.05$). Generally, sites with wastewater discharge had a significantly higher EF than those without wastewater discharge (Fig. 4f).

Over the study period, the EF value ranged from 1.8×10^{-3}–6.0×10^{-3} in the river, 2.0×10^{-3}–5.4×10^{-3} in the drainage channels, 2.1×10^{-3}–7.4×10^{-3} in the aquaculture ponds and 1.4×10^{-3}–2.6×10^{-3} in the reservoir (Fig. 5). The EF value varied significantly among the four water types (ANOVA, $p < 0.001$; Table 1) and the respective means (±SEs) were $3.3\times10^{-3} \pm 1.4\times10^{-3}$ (river), $3.2\times10^{-3} \pm 1.1\times10^{-3}$ (drainage channels), $4.5\times10^{-3} \pm 1.5\times10^{-3}$ (aquaculture ponds) and $1.8\times10^{-3} \pm 0.4\times10^{-3}$ (reservoir).

EF also varied significantly between seasons ($p < 0.001$; Table 1). The highest EF was recorded in the summer months in all areas, in some cases more than two-fold above the autumn and spring months (Fig. 5).

3.4. Relationships between EF and environmental variables

EF across all sampling sites was correlated linearly with T_W ($r^2 = 0.61$; $p < 0.01$; Fig. 6a). EF also correlated significantly with DOC but in an exponential manner ($r^2 = 0.93$; $p < 0.01$; Fig. 6b). When plotted against DOC:NO_3^-–N, a linear relationship is obtained ($r^2 = 0.84$; $p < 0.01$; Fig. 6c). In contrast, EF was negatively but weakly correlated with EC (Fig. 6d) and NO_3^-–N concentration (Fig. 6e) ($r^2 = 0.26$–0.27; $p < 0.05$). We found

231 a significant and negative correlation between salinity and EF across the different
232 months (p<0.01; Fig. 7a-c), and the combined data show an exponential decrease in EF
233 with increasing salinity (r^2 = 0.41; p<0.01; Fig. 7d). No significant correlation was
234 found between EF and pH, DO, COD or TDN (p > 0.05).

235 ## 4. Discussion

236 *4.1. N_2O distribution in coastal reservoir and its catchment*

237 Given its powerful warming effect, proper assessment and mitigation of N_2O is
238 critical for nations to meet their commitment to combat global warming (IPCC, 2018).
239 The "top-down" approach focuses on the outcome of increasing production and
240 emission of N_2O by measuring the changes in atmospheric N_2O level. However, in
241 order for nations to devise and implement policies to curb N_2O emission, it is necessary
242 to use "bottom-up" approach to identify and quantify the sources of N_2O (Del Grosso et
243 al., 2008). Notwithstanding its limitation, EF remains an indispensable tool for
244 bottom-up N_2O assessments because of its ability to encapsulate the complex aquatic
245 nitrogen biogeochemical processes into easily quantifiable parameters, such as NO_3^--N.
246 However, for urbanized coastal reservoirs that receive water and nutrient inputs from
247 multiple sources across a heterogeneous landscape, applying a fixed EF value may
248 translate to large errors in N_2O assessments. For improvement, we seek to refine and
249 constrain EF by considering the high-resolution distribution of N_2O and its
250 environmental driver(s).

251 We observed considerable variations in N_2O concentration in the four surface

water types. N_2O level was similarly low across all water types in the autumn month, but it reached significantly higher levels in the summer month—more than double in the river and aquaculture ponds (Fig. 3). Interestingly, both NO_3^--N and TDN concentrations were lower in the summer (Fig. 2g). This suggests that the higher summer-time N_2O was not caused by a higher amount of N substrates. Rather, the large summer-time increase could be attributed to the higher water temperature (Fig. 2a) increasing microbial transformation of N to N_2O (McMahon and Dennehy 1999; Tian et al., 2017, 2018). Nevertheless, because the seasonal temperature change was nearly identical across all sampling sites, temperature alone could not explain the spatial differences in N_2O among the different water types. Also, the observation that N_2O spatiotemporal variations were disconnected from NO_3^--N and TDN further highlights the existence of moderating factors in N_2O production and the deficiency in using a fixed EF value.

4.2. Environmental influence of EF

It is clear from the data that EF varied substantially in space and in time in the reservoir. We observed considerably higher EF in the north basin than in the south basin of the reservoir (Fig. 4), which may be attributed to the different hydrographical properties between the two basins that influenced N_2O production. Salinity is higher in SB due to its close proximity to the sea (Yang et al., 2020). Previous research has shown that high salinity could adversely impact the abundance and activity of ammonia-oxidizing bacteria (Li et al., 2021; Mosier and Francis, 2008; Neubauer et al.,

273 2019), thereby decreasing N_2O production and emission (Liu et al., 2015; Wang et al.,
274 2018; Welti et al., 2017). Similarly, we found a significant and negative correlation
275 between salinity and EF across the entire data set (Fig. 7), indicating that seawater
276 intrusion is an important factor moderating N_2O production. Alternatively, the
277 relationship could suggest low N_2O seawater mixing and diluting with higher N_2O
278 freshwater. Furthermore, the north basin is situated in an area with intensive human
279 activity and it receives sewage discharge and river inflows, leading to higher microbial
280 and substrate loading that could potentially increase N_2O production as compared to the
281 south basin. This is consistent with the observations that EF was higher in NB and in
282 sites impacted by wastewater (Fig. 4a and 4b).

283 The common formulations of EF are functions of nitrogen in the form of total N
284 input or NO_3^--N, based on the idea that increase in those should proportionally increase
285 N_2O. However, we found that EF correlated negatively (albeit weakly) with NO_3^--N
286 (Fig. 6e), as also reported for artificial surface waters (Webb et al., 2021), suggesting
287 that NO_3^--N alone is a poor predictor of N_2O in the system. The large spatial and
288 temporal variations in EF also mean that using a fixed EF would inevitably lead to
289 errors when assessing N_2O emission. For example, our empirically derived EF deviated
290 from the IPCC (2019) default EF value in all surface water types and all sampling
291 months (Fig. 5). On average, the IPCC default EF of 2.6×10^{-3} would overestimate N_2O
292 emission from the reservoir but underestimate N_2O emissions from the adjacent river,
293 drainage channels and aquaculture ponds, sometimes by as much as 42%.

294 *4.3. Improving EF with hydrographical parameters*

295 The application of emission factor (EF) offers important practical convenience in
296 greenhouse gas accounting at the national level. However, the biogeochemical
297 processes that lead to N_2O production and emission can be complex and variable at the
298 local level, which cannot be encapsulated realistically by a fixed EF value. Some
299 researchers have criticized the IPCC default EF for grossly overestimating N_2O
300 emissions (e.g. Hu et al., 2017; Kuang et al., 2021; Maavara et al., 2019). Likewise, our
301 results showed that the IPCC default EF tends to underestimate emission from waters
302 with a high DOC:NO_3^-–N. With the DOC:NO_3^-–N ratio trending upward in many
303 inland water bodies as a result of changing catchment processes (Weyhenmeyer and
304 Jeppesen, 2010), it is necessary to continuously revise and improve EF for more proper
305 N_2O emission assessments.

306 We examined the empirical relationships between EF and hydrographical
307 parameters in order to derive better algorithms for EF. Among the parameters we
308 investigated, EF correlated negatively with EC and NO_3^-–N, but the corrections were
309 weak (r^2 = 0.11-0.49; Fig. 6 d-e), which we consider not suitable for practical use.
310 Water temperature is a most basic parameter in environmental monitoring and it affects
311 a multitude of biogeochemical processes; water temperature data are also widely
312 available in databases. Our study showed a significant linear relationship between EF
313 and surface water temperature (T_W) across a range (18-29 °C) typical for subtropical
314 environments (Fig. 6a). Scientists may therefore substitute the IPCC default EF with a

315 temperature-dependent EF to improve N_2O assessments, with the caveat that the
316 predictive model has only a moderate r^2 (0.54). This temperature-dependent algorithm
317 can be improved with more measurements including higher temperatures from the
318 tropical region and lower temperatures such as the winter month and higher latitudes.

319 While NO_3^-–N is the precursor of N_2O, the biochemical transformation of N still
320 requires the work of microbes including denitrifying bacteria, which in turns rely on
321 dissolved organic carbon (DOC) as the energy source (Holmes et al., 1996; Stow et al.,
322 2005; Schipper et al., 2010). As such, one may derive an algorithm to incorporate DOC
323 as a surrogate indicator of microbial activity. Indeed, our observations showed that EF
324 correlated significantly ($p < 0.01$) with DOC as described by an exponential equation,
325 with a high r^2 of 0.84 (Fig. 6b). As DOC is a basic environmental monitoring parameter,
326 the new algorithm provides an easy way to adjust and improve EF with DOC data.
327 However, further consideration is needed when applying this algorithm elsewhere.
328 DOC concentration in inland waters varies widely and can reach up to 300 mg L^{-1} in
329 hypereutrophic waters (Sobek et al., 2007), whereas our measurements cover a rather
330 narrow range of DOC. If we were to extrapolate the algorithm forward, it would give an
331 unrealistic EF at higher DOC concentrations. As such, despite the high r^2 (0.84),
332 application of this algorithm should be limited to coastal reservoirs with a similar DOC
333 concentration range.

334 A simple improvement to the algorithm is by adding NO_3^-–N as an additional
335 constraining variable. In inland waters including ones impacted by anthropogenic

activities, DOC is often coupled to N input such that the DOC:NO_3^-–N ratio tends to vary within a relatively narrow range. In our study, we observed a significant linear relationship between EF and DOC:NO_3^-–N despite a slightly lower r^2 value (0.83) (Fig. 6c). The DOC:NO_3^-–N (mg/mg) range in our data covers most of the DOC:NO_3^-–N values reported for inland waters (Weyhenmeyer and Jeppesen, 2010; Heppell et al., 2017). As such, an algorithm based on DOC:NO_3^-–N provides another useful tool to derive EF for N_2O emission from coastal reservoirs and their catchments.

Lastly, considering that both T_W and DOC:NO_3^-–N show good correlations with EF, we derived a new algorithm with both independent variables in a multiple regression analysis. The resultant equation is:

$$EF = -0.001 + 0.00007\ T_W + 0.00041\ DOC{:}NO_3^-N \quad \text{(Eq. 1)}$$

The two independent variables, when combined in Eq. 1, also give a significant and high explanatory power ($F = 32.24$, $r^2 = 0.82$, $p < 0.001$). We therefore consider this new algorithm most preferred and ecologically relevant because it incorporates the effects of the three key environmental drivers by relating the variability of EF to the influences of hydrographical condition (T_W) and N_2O precursor (NO_3^--N) as moderated by microbial activity (with DOC as the surrogate indicator).

5. Conclusions

The trade-off between convenience and accuracy in N_2O assessment based on IPCC-default EF has important ramifications as nations strive to improve greenhouse

gas mitigations and climate change policies. We found that EF varied temporally and spatially in a complex and dynamic system such as a coastal reservoir that was influenced by multiple input sources; therefore, applying the IPCC default EF could lead to error in N_2O emission assessment, sometimes by as much as 42%. The observed EF was significantly related to surface water temperature, dissolved organic carbon and nitrate concentrations; therefore, an algorithm based on the three hydrographical parameters combined could be used to derive a EF to improve N_2O emission from urbanized coastal reservoirs. Further improvement will require more data to test its application in other aquatic systems.

Declaration of competing interest

The authors declare that they have no known competing financial interests or personal relationships that could have appeared to influence the work reported in this paper.

Acknowledgements

This research was supported by the National Science Foundation of China (No. 41801070, 41671088), the National Science Foundation of Fujian Province (No. 2020J01136, 2019J05067), the Minjiang Scholar Programme. We would like to thank Yifei Zhang, Chen Tang, Guanghui Zhao and Ling Li of the School of Geographical Sciences, Fujian Normal University, for their field assistance. ~~The data used in this study are available in the Supplementary Material file.~~

References

Beaulieu, J.J., Tank, J.L., Hamilton, S.K., Wollheim, W.M., Hall Jr., R.O., Mulholland, P.J., Peterson, B.J., Ashkenas, L.R., Cooper, L.W., Dahm, C.N., Dodds, W.K., Grimm, N.B., Johnson, S.L., McDowell, W.H., Poole, G.C., Valett, H.M., Arango, C.P., Bernot, M.J., Burgin, A.J., Crenshaw, C.L., Helton, A.M., Johnson, L.T., O'Brien, J.M., Potter, J.D., Sheibley, R.W., Sobota, D.J., Thomas, S.M., 2011. Nitrous oxide emission from denitrification in stream and river networks. PNAS 108, 214−219. https://doi.org/10.1073/pnas.1011464108

Borges, A.V., Speeckaert, G., Champenois, W., Scranton, M.I., Gypens, N., 2018. Productivity and temperature as drivers of seasonal and spatial variations of dissolved methane in the Southern Bight of the North Sea. Ecosystems 21(4), 583−599. https://doi.org/10.1007/s10021-017-0171-7.

Brase, L., Bange, H.W., Lendt, R., Sanders, T., Dähnke, K., 2017. High resolution measurements of nitrous oxide (N_2O) in the Elbe Estuary. Front. Mar. Sci. 4, 162. https://doi.org/10.3389/fmars.2017.00162

Ciais, P., Sabine, C., Bala, G., Bopp, L., Brovkin, V., Canadell, J., Chhabra, A., DeFries, R., Galloway, J., Heimann, M., Jones, C., Le Quere, C., Myneni, R.B., Piao, S., Thornton, P. 2014. Carbon and Other Biogeochemical Cycles. Climate Change 2013: the Physical Science Basis. Contribution of Working Group I to the Fifth Assessment Report of the Intergovernmental Panel on Climate Change.; Stocker, T.F., Qin, D., Plattner, G.-K., Tignor, M., Allen, S.K., Boschung, J., Nauels, A., Xia, Y., Bex, V., Midgley, P.M., Eds.; Cambridge University Press, pp. 465–570.

Cooper, R.J., Wexler, S.K., Adams, C.A., Hiscock, K.M., 2017. Hydrogeological controls on regional-scale indirect nitrous oxide emission factors for rivers. Environ. Sci. Technol. 51, 10440-10448. http://dx.doi.org/10.1021/acs.est.7b02135

Davidson, E.A., 2009. The contribution of manure and fertilizer nitrogen to atmospheric nitrous oxide since 1860. Nat. Geosci. 2, 659-662. https://doi.org/10.1038/ngeo608

Davidson, T.A., Audet, J., Svenning, J.- C., Lauridsen, T.L., Søndergaard, M., Landkildehus, F., Larsen, S.E., Jeppesen, E., 2015. Eutrophication effects on greenhouse gas fluxes from shallow-lake mesocosms override those of climate warming. Global Change Biol. 21, 4449−4463. https://doi.org/10.1111/gcb.13062

De Klein, C., Novoa, R.S.A., Ogle, S., Smith, K.A., Rochette, P., Wirth, T.C., 2006. N_2O emissions from managed soils, and CO_2 emissions from lime and urea application. In 2006 IPCC guidelines for national greenhouse gas inventories. Cambridge University Press, Cambridge, pp, 54.

Del Grosso, S.J., Wirth, T., Ogle, S.M., Parton, W.J., 2008. Estimating agricultural nitrous oxide emissions. Eos Trans. AGU 89(51), 529–529. https://doi.org/10.1029/2008EO510001

Fu, C., Lee, X., Griffis, T.J., Baker, J. M., Turner, P.A., 2018. A modeling study of direct and indirect N_2O emissions from a representative catchment in the U.S. Corn Belt. Water Resour. Res. 54(5), 3632−3653. https://doi.org/10.1029/2017WR022108

Griffis, T.J., Lee, X., Baker, J.M., Russelle, M.P., Zhang, X., Venterea, R., Millet, D.B., 2013. Reconciling the differences between top-down and bottom-up estimates of nitrous oxide emissions for the U.S. Corn Belt. Global Biogeochem. Cy. 27(3), 746–754. https://doi.org/10.1002/gbc.20066

Hama-Aziz, Z.Q., Hiscock, K.M., Cooper, R.J., 2017. Indirect nitrous oxide emission factors for agricultural field drains and headwater streams. Environ. Sci. Technol. 51, 301–307. https://doi.org/10.1021/acs.est.6b05094

Heppell, C.M., Binley, A., Trimmer, M., Darch, T., Jones, A., Malone, E., Collins, A.L., Johnes, P.J., Freer, J.E., Lloyd, C.E.M., 2017. Hydrological controls on DOC:nitrate resource stoichiometry in a lowland, agricultural catchment, southern UK. Hydrol. Earth Syst. Sci. 21(9), 4785–4802. https://doi.org/10.5194/hess-21-4785-2017

Herrman, K.S., Bouchard, V., Moore, R.H., 2008. Factors affecting denitrification in

agricultural headwater streams in Northeast Ohio, USA. Hydrobiologia 598, 305–314. https://doi.org/10.1007/s10750-007-9164-4

Hinshaw, S.E., Dahlgren, R.A., 2013. Dissolved nitrous oxide concentrations and fluxes from the eutrophic San Joaquin River, California. Environ. Sci. Technol. 47, 1313–1322. https://doi.org/10.1021/es301373h

Holmes, R.M., Jones, J.B., Fisher, S.G., Grimm, N.B., 1996. Denitrification in a nitrogen-limited stream ecosystem. Biogeochemistry 33, 125–146.

Hu, M., Chen, D., Dahlgren, R. A., 2016. Modeling nitrous oxide emission from rivers: a global assessment. Global Change Biol. 22(11), 3566–3582. https://doi.org/10.1111/gcb.13351

IPCC, 2006. IPCC Guidelines for National Greenhouse Gas Inventories Prepared by the National Greenhouse Gas Inventories Programme; Eggleston, H. S., Buendia, L., Miwa, K., Ngara, T., Tanabe, K., Eds.; IGES: Japan, 2006.

IPCC, 2018. Global Warming of 1.5°C. [Masson-Delmotte, V., et al.]. https://www.ipcc.ch/site/assets/uploads/sites/2/2019/06/SR15_Full_Report_High_Res.pdf

IPCC, 2019. In: Calvo Buendia, E., Tanabe, K., Kranjc, A., Baasansuren, J., Fukuda, M., Ngarize, S., Osako, A., Pyrozhenko, Y., Shermanau, P., Federici, S. (Eds.), 2019 Refinement to the 2006 IPCC Guidelines for National Greenhouse Gas Inventories, Volum 4. IPCC, Switzerland, Kanagawa, JAPAN. Chapter 11.

Jurado, A., Borges, A.V., Brouyere, S., 2017. Dynamics and emissions of N_2O in groundwater: a review. Sci. Total Environ. 584, 207–218. https://doi.org/10.1016/j.scitotenv.2017.01.127

Kroeze, C., Dumont, E., Seitzinger, S., 2010. Future trends in emissions of N_2O from rivers and estuaries. J. Integr. Environ. Sci. 7, 71–78. https://doi.org/10.1080/1943815x.2010.49678

Kuang, W.N., Gao, X.P., Tenuta, M., Zeng, F.J., 2021. A global meta- analysis of nitrous oxide emission from drip- irrigated cropping system. Global Change Biol.

https://doi.org/10.1111/gcb.15636

Lacerda, L.D., Molisani, M.M., Sena, D., Maia, L.P., 2008. Estimating the importance of natural and anthropogenic sources on N and P emission to estuaries along the Ceará state coast NE Brazil. Environ. Monit. Assess. 141, 149−164. https://doi.org/10.1007/s10661-007-9884-y

Li, X.F., Qian, W., Hou, L.J., Liu, M., Chen, Z.B., Tong, C., 2021. Human activity intensity controls the relative importance of denitrification and anaerobic ammonium oxidation across subtropical estuaries. Catena 202, 105260. https://doi.org/10.1016/j.catena.2021.105260.

Liu, X.L., Bai, L., Wang, Z.L., Li, J., Yue, F.J., Li, S.L., 2015. Nitrous oxide emissions from river network with variable nitrogen loading in Tianjin, China. J. Geochem. Explor. 157, 153−161. https://doi.org/10.1016/j.gexplo.2015.06.009

Liu, X.L., Liu, C.Q., Li, S.L., Wang, F.S., Wang, B.L., Wang, Z.L., 2011. Spatiotemporal variations of nitrous oxide (N_2O) emissions from two reservoirs in SW China. Atmos. Environ. 45 (31), 5458−5468. https://doi.org/10.1016/j.atmosenv.2011.06.074

Liu, X.L., Li, S.L., Wang, Z.L., Han, G.L., Li, J., Wang, B.L., Wang, F.S., Bai, L., 2017. Nitrous oxide (N_2O) emissions from a mesotrophic reservoir on the Wujiang River, southwest China. Acta Geochim. 36(4), 667−679. https://doi.org/10.1007/s11631-017-0172-4

Maavara, T., Lauerwald, R., Laruelle, G.G., Akbarzadeh, Z., Bouskill, N.J., Van Cappellen, P., Regnier, P., 2019. Nitrous oxide emissions from inland waters: Are IPCC estimates too high? Glob Change Biol. 25, 473–488. https://doi.org/10.1111/gcb.14504

McMahon, P.B., Dennehy K.F., 1999. N_2O emissions from a nitrogenenriched river. Environ. Sci. Technol. 33, 21–25. https://doi.org/10.1021/es980645n

Moin, N.S., Nelson, K.A., Bush, A., Bush, A., Bernhard, A.E., 2009. Distribution and diversity of archaeal and bacterial ammonia oxidizers in salt marsh sediments.

Appl. Environ. Microbiol. 7(23), 7461–7468. https://doi.org/10.1128/AEM.01001-09

Mosier, A.C., Francis, C.A., 2008. Relative abundance and diversity of ammonia-oxidizing archaea and bacteria in the San Francisco Bay estuary. Environ. Microbiol. 10(11), 3002–3016. https://doi.org/10.1111/j.1462-2920.2008.01764.x

Mosier, A., Kroeze, C., Nevison, C., Oenema, O., Seitzinger, S., van Cleemput, O., 1998. Closing the global N_2O budget: nitrous oxide emissions through the agricultural nitrogen cycle. Nutr. Cycl. Agroecosys. 52, 225–248.

Neubauer, S.C., Megonigal, J.P., 2015. Moving beyond global warming potentials to quantify the climatic role of ecosystems. Ecosystems, 18(6), 1000-1013. https://doi.org/10.1007/s10021-015-9879-4

Neubauer, S.C., Piehler, M.F., Smyth, A.R., Franklin, R.B., 2019. Saltwater intrusion modifies microbial community structure and decreases denitrification in tidal freshwater marshes. Ecosystems 22 (4), 912–928. https://doi.org/10.1007/s10021-018-0312-7

Outram, F.N., Hiscock, K.M., 2012. Indirect nitrous oxide emissions from surface water bodies in a lowland arable catchment: a significant contribution to agricultural greenhouse gas budgets? Environ. Sci. Technol. 46(15), 8156–8163. https://doi.org/10.1021/es3012244

Páez-Osuna, F., Álvarez-Borrego, S., Ruiz-Fernández, A.C., García-Hernández, J., JaraMarini, M.E., Bergés-Tiznado, M.E., Piñón-Gimate, A., Alonso-Rodríguez, R., SotoJiménez, M.F., Frías-Espericueta, M.G., Ruelas-Inzunza, J., Green-Ruiz, C.R., OsunaMartínez, C.C., Sánchez-Cabeza, J.A., 2017. Environmental status of the Gulf of California: a pollution review. Earth-Sci. Rev. 166, 181–205. https://doi.org/10.1016/j.earscirev.2017.01.014

Phanwilai, S., Kangwannarakul, N., Noophan, P., Kasahara, T., Terada, A., Munakata-Marr, J., and Figueroa, L.A., 2020. Nitrogen removal efficiencies and

517 microbial communities in full-scale IFAS and MBBR municipal wastewater
518 treatment plants at high COD:N ratio. Front. Environ. Sci. Eng. 14(6), 115.
519 https://doi.org/10.1007/s11783-020-1374-2
520 Qin, X.B., Li, Y., Goldberg, S., Wan, Y.F., Fan, M.R., Liao, Y.L., Wang, B., Gao, Q.Z.,
521 Li, Y.E., 2019. Assessment of indirect N_2O emission factors from agricultural river
522 networks based on long-term study at high temporal resolution. Environ. Sci.
523 Technol. 53, 10781–10791. https://doi.org/10.1021/acs.est.9b03896
524 Quick, A.M., Reeder, W.J., Farrell, T.B., Tonina, D., Feris, K.P., Benner, S.G., 2019.
525 Nitrous oxide from streams and rivers: a review of primary biogeochemical
526 pathways and environmental variables. Earth Sci. Rev. 191, 224–262.
527 https://doi.org/10.1016/j.earscirev.2019.02.021
528 Ravishankara, A.R., Daniel, J.S., Portmann, R.W., 2009. Nitrous oxide (N_2O): the
529 dominant ozone-depleting substance emitted in the 21st century. Science 326,
530 123–125. https://doi.org/10.1126/science.1176985
531 Saikawa, E., Prinn, R.G., Dlugokencky, E., Ishijima, K., Dutton, G.S., Hall, B.D.,
532 Langenfelds, R., Tohjima, Y., Machida, T., Manizza, M., Rigby, M., O'Doherty, S.,
533 Patra, P.K., Harth, C.M., Weiss, R.F., Krummel, P.B., van der Schoot, M., Fraser,
534 P.J., Steele, L.P., Aoki, S., Nakazawa,T., Elkins, J.W., 2014. Global and regional
535 emissions estimates for N_2O. Atmos. Chem. Phys. 14, 4617–4641.
536 https://doi.org/10.5194/acp-14-4617-2014
537 Schreiber, F., Wunderlin, P., Udert, K. M., Wells, G. F., 2012. Nitric oxide and nitrous
538 oxide turnover in natural and engineered microbial communities: biological
539 pathways, chemical reactions, and novel technologies. Front. Microbiol. 3, 372.
540 https://doi.org/10.3389/fmicb.2012.00372
541 Sobek, S., Tranvik, L.J., Prairie, Y.T., Kortelainen, P., Cole, J.J., 2007. Patterns and
542 regulation of dissolved organic carbon: An analysis of 7,500 widely distributed
543 lakes. Limnol. Oceanogr. 52(3), 1208-1219.
544 https://doi.org/10.4319/lo.2007.52.3.1208

Stow, C.A., Walker, J.T., Cardoch, L., Spence, P., Geron, C., 2005. N_2O emissions from streams in the Neuse River Watershed, North Carolina. Environ. Sci. Technol. 39, 6999–7004. https://doi.org/10.1021/es0500355

Syakila, A., Kroeze, C., 2011. The global nitrous oxide budget revisited. Greenhouse Gas Meas. Manage. 1, 17−26. https://doi.org/10.3763/ghgmm.2010.0007

Tian, H.Q., Xu, R.T., Canadell, J.G., Thompson, R.L., Winiwarter, W., Suntharalingam, P., Davidson, E.A., Ciais, P., Jackson, R.B., Janssens-Maenhout, G., Prather, M.J., Regnier, P., Pan, N.Q., Pan, S.F., Peters, G.P., Shi, H., Tubiello, F.N., Zaehle, S., Zhou, F., Arneth, A., Battaglia, G., Berthet, S., Bopp, L., Bouwman, A.F., Buitenhuis, E.T., Chang, J.F., Chipperfield, M.P., Dangal, S.R.S., Dlugokencky, E., Elkins, J.W., Eyre, B.D., Fu, B.J., Hall, B., Ito, A., Joos, F., Krummel, P.B., Landolfi, A., Laruelle, G.G., Lauerwald, R., Li, W., Lienert, S., Maavara, T., MacLeod, M., Millet, D.B., Olin, S., Patra, P.K., Prinn, R.G., Raymond, P.A., Ruiz, D.J., van der Werf, G.R., Vuichard, N., Wang, J.J., Weiss, R.F., Wells, K.C., Wilson, C., Yang, J., Yao, Y.Z., 2020. A comprehensive quantification of global nitrous oxide sources and sinks. Nature 586(7828), 248−256. https://doi.org/10.1038/s41586-020-2780-0

Tian, L.L., Akiyama, H., Zhu, B., Shen, X., 2018. Indirect N_2O emissions with seasonal variations from an agricultural drainage ditch mainly receiving interflow water. Environ. Pollut. 242, 480-491. https://doi.org/10.1016/j.envpol.2018.07.018

Tian, L.L., Zhu, B., Akiyama, H., 2017. Seasonal variations in indirect N_2O emissions from an agricultural headwater ditch. Biol. Fert. Soils 53, 651−662. https://doi.org/10.1007/s00374-017-1207-z

Turner, P.A., Griffis, T.J., Lee, X., Baker, J.M., Venterea, R.T., Wood, J.D., 2015. Indirect nitrous oxide emissions from streams within the US Corn Belt scale with stream order. PNAS 112, 9839−9843. https://doi.org/10.1073/pnas.1503598112

Wang, X.M., Hu, M.J., Ren, H.C., Li, J.B., Tong, C., Musenze, R.S., 2018. Seasonal variations of nitrous oxide fluxes and soil denitrification rates in subtropical

freshwater and brackish tidal marshes of the Min River estuary. Sci. Total Environ. 616–617, 1404–1413. https://doi.org/10.1016/j.scitotenv.2017.10.175

Wanyama, I., Rufino, M.C., Pelster, D.E., Wanyama, G., Atzberger, C., van Asten, P., Verchot, L.V., Butterbach-Bahl, K., 2018. Land use, land use history, and soil type affect soil greenhouse gas fluxes from agricultural landscapes of the east african highlands. J. Geophys. Res.-Biogeo. 123, 976−990. https://doi.org/10.1002/2017JG003856

Webb, J.R., Clough, T.J., Quayle, W.C., 2021. A review of indirect N_2O emission factors from artificial agricultural waters. Environ. Res. Lett. 16, 043005. https://doi.org/10.1088/1748-9326/abed00

Welti, N., Hayes, M., Lockington, D., 2017. Seasonal nitrous oxide and methane emissions across a subtropical estuarine salinity gradient. Biogeochemistry 132, 55–69. https://doi.org/10.1007/s10533-016-0287-4

Weiss, R.F., Price, B.A. 1980. Nitrous oxide solubility in water and seawater. Mar. Chem. 8(4), 347−359. https://doi.org/10.1016/0304-4203(80)90024-9

Weyhenmeyer, G.A., Jeppesen, E., 2010. Nitrogen deposition induced changes in DOC:NO_3^-–N ratios determine the efficiency of nitrate removal from freshwaters. Global Change Biol. 16(8), 2358–2365. https://doi.org/10.1111/j.1365-2486.2009.02100.x

National Oceanic and Atmospheric, 2021. Carbon cycle greenhouse gases: Trends in Atmospheric Nitrous Oxide. Available in: https://gml.noaa.gov/ccgg/trends_n2o/

Xiao, Q.T., Hu, Z.H., Fu, C.S., Bian, H., Lee, X.H., Chen, S.T., Shang, D.Y., 2019a. Surface nitrous oxide concentrations and fluxes from water bodies of the agricultural watershed in Eastern China. Environ. Pollut. 251, 185–192. https://doi.org/10.1016/j.envpol.2019.04.076

Xiao, Q.T., Xu, X.F., Zhang, M., Duan, H.T., Hu, Z.H., Wang, W., Xiao, W., Lee, X.H., 2019b. Coregulation of nitrous oxide emissions by nitrogen and temperature in China's third largest freshwater lake (Lake Taihu). Limnol. Oceanogr. 64, 1070–

1086. https://doi.org/10.1002/lno.11098

Yang, P., Yang, H., Sardans, J., Tong, C., Zhao, G.H., Peñuelas, J., et al., 2020. Large spatial variations in diffusive CH_4 fluxes from a subtropical coastal reservoir affected by sewage discharge in southeast China. Environ. Sci. Technol. 54, 22, 14192–14203. https://doi.org/10.1021/acs.est.0c03431

Yang, P., Lu, M.H., Tang, K.W., Yang, H., Lai, D.Y.F., Tong, C., Chun, K.P., Zhang, L.H., Tang, C., 2021. Coastal reservoirs as a source of nitrous oxide: spatio-temporal patterns and assessment strategy. Sci. Total Environ. 147878. https://doi.org/10.1016/j.scitotenv.2021.147878

Yang, S.Q., 2018. Coastal reservoir—How to develop freshwater from the sea without desalination. In: Water resources management. Springer, Singapore, 121-139.

Yu, Z.J., Deng, H.G., Wang, D.Q., Ye, M.W., Tan, Y.J., Li, Y.J., Chen, Z.L., Xu, S.Y., 2013. Nitrous oxide emissions in the Shanghai river network: implications for the effects of urban sewage and IPCC methodology. Global Change Biol. 19, 2999–3010. https://doi.org/10.1111/gcb.12290

Zhang, L., Wang, L., Yin, K.D., Lü, Y., Zhang, D.R., Yang, Y.Q., Huang, X.P., 2013. Pore water nutrient characteristics and the fluxes across the sediment in the Pearl River estuary and adjacent waters, China. Estuar. Coast. Shelf S.133, 182–192. https://doi.org/10.1016/j.ecss.2013.08.028

Zhang, W.S., Li, H.P., Xiao, Q.T., Jiang, S.Y., Li, X.Y., 2020. Surface nitrous oxide (N_2O) concentrations and fluxes from different rivers draining contrasting landscapes: Spatio-temporal variability, controls, and implications based on IPCC emission factor. Environ. Pollut. 263, 114457. https://doi.org/10.1016/j.envpol.2020.114457

Zhang Y.F., Lyu M., Yang P., Lai D.Y.F., Tong C., Zhao G.H., Li L., Zhang Y.H., Yang, H., 2021. Spatial variations in CO_2 fluxes in a subtropical coastal reservoir of Southeast China were related to urbanization and land-use types. J. Environ. Sci. 109, 206–218. https://doi.org/10.1016/j.jes.2021.04.003

Author Contribution Statement

Conceptualization: Ping Yang, Chuan Tong, Kam W. Tang

Methodology: Ping Yang, Chuan Tong,

Formal analysis: Ping Yang, Kam W. Tang

Validation: Ping Yang

Investigation: Ping Yang, Liangjuan Luoa, Yan Hong, Linhai Zhang

Data Curation: Ping Yang

Writing-Original Draft: Ping Yang, Chuan Tong, Kam W. Tang, Derrick Y. F. Lai

Writing - Review & Editing: Chuan Tong, Derrick Y. F. Lai, Kam W. Tang

Project Administration: Ping Yang, Chuan Tong

Funding acquisition: Ping Yang, Chuan Tong

Graphical Abstract

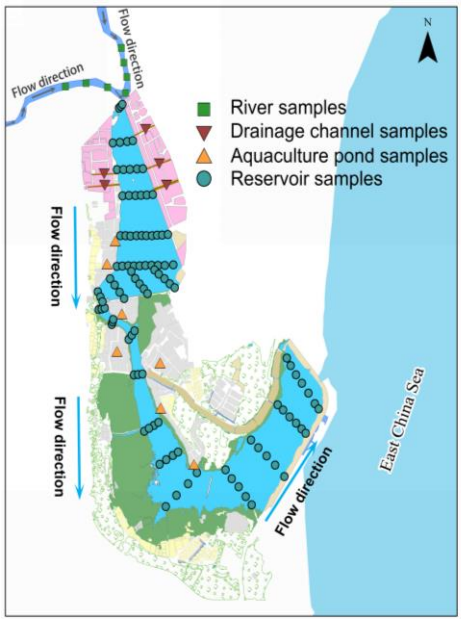

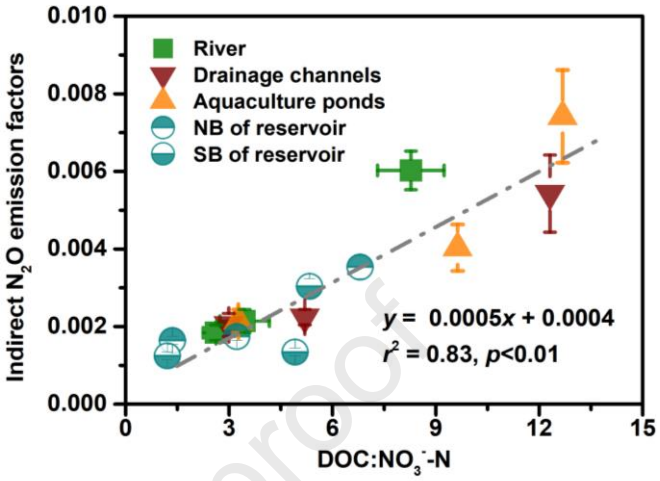

Table 1 Results of two-way ANOVAs examining the effect of sampling area, season and their interactions on dissolved N_2O concentration and N_2O emission factor (EF).

	df	**Dissolved N_2O concentration**				**N_2O emission factor (EF)**			
		Sum of squares	*Mean square*	*F value*	*P value*	*Sum of squares*	*Mean square*	*F value*	*P value*
Sampling area	3	107882.38	35960.79	24.46	<0.01	1.88	0.63	36.30	<0.01
Season	2	61674.53	30837.27	20.98	<0.01	2.09	1.04	60.33	<0.01
Sampling area × Season	6	59233.93	9872.32	6.70	<0.01	0.96	0.16	9.26	<0.01
Residuals		515961.43	1469.98			6.07	0.02		

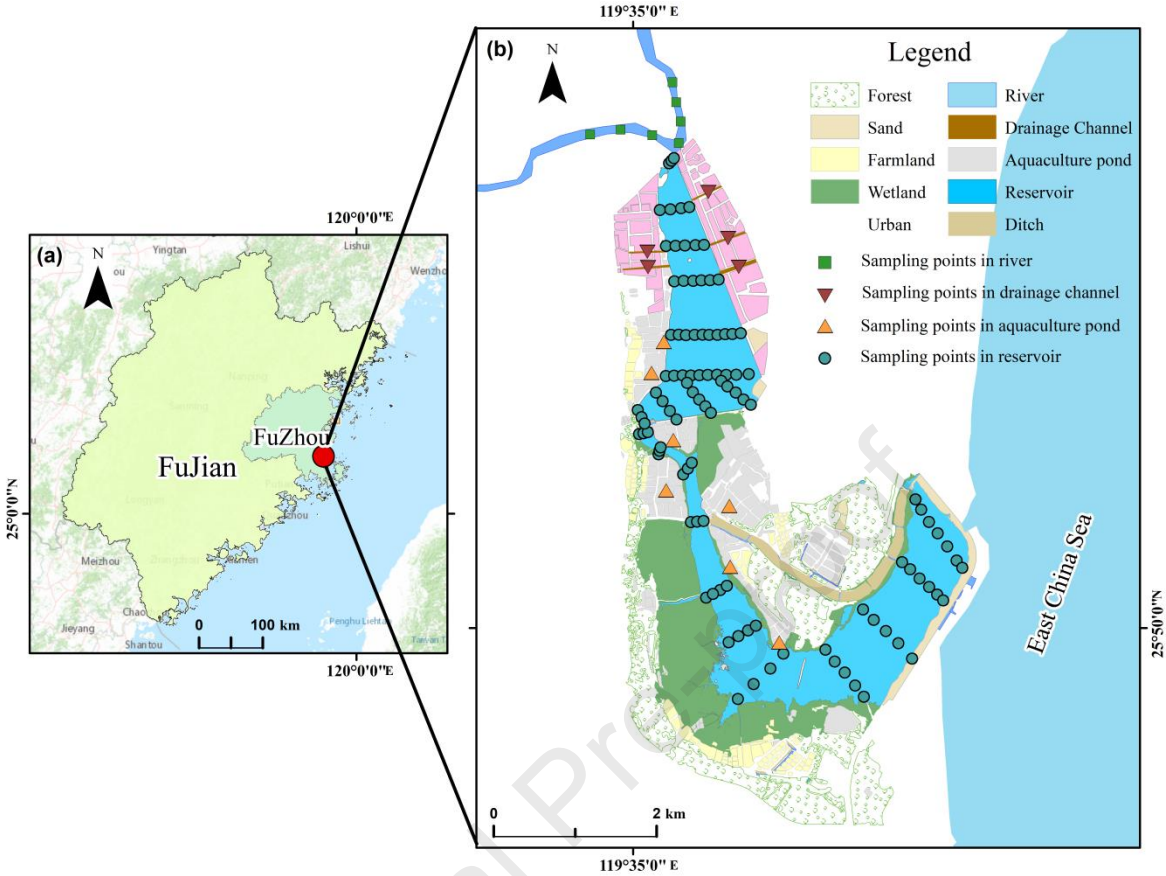

Fig. 1. Location of (a) the study areas and (b) sampling sites in the Wenwusha Reservoir and the adjacent areas (river, drainage channels, aquaculture ponds) in Fujian Province, southeastern China.

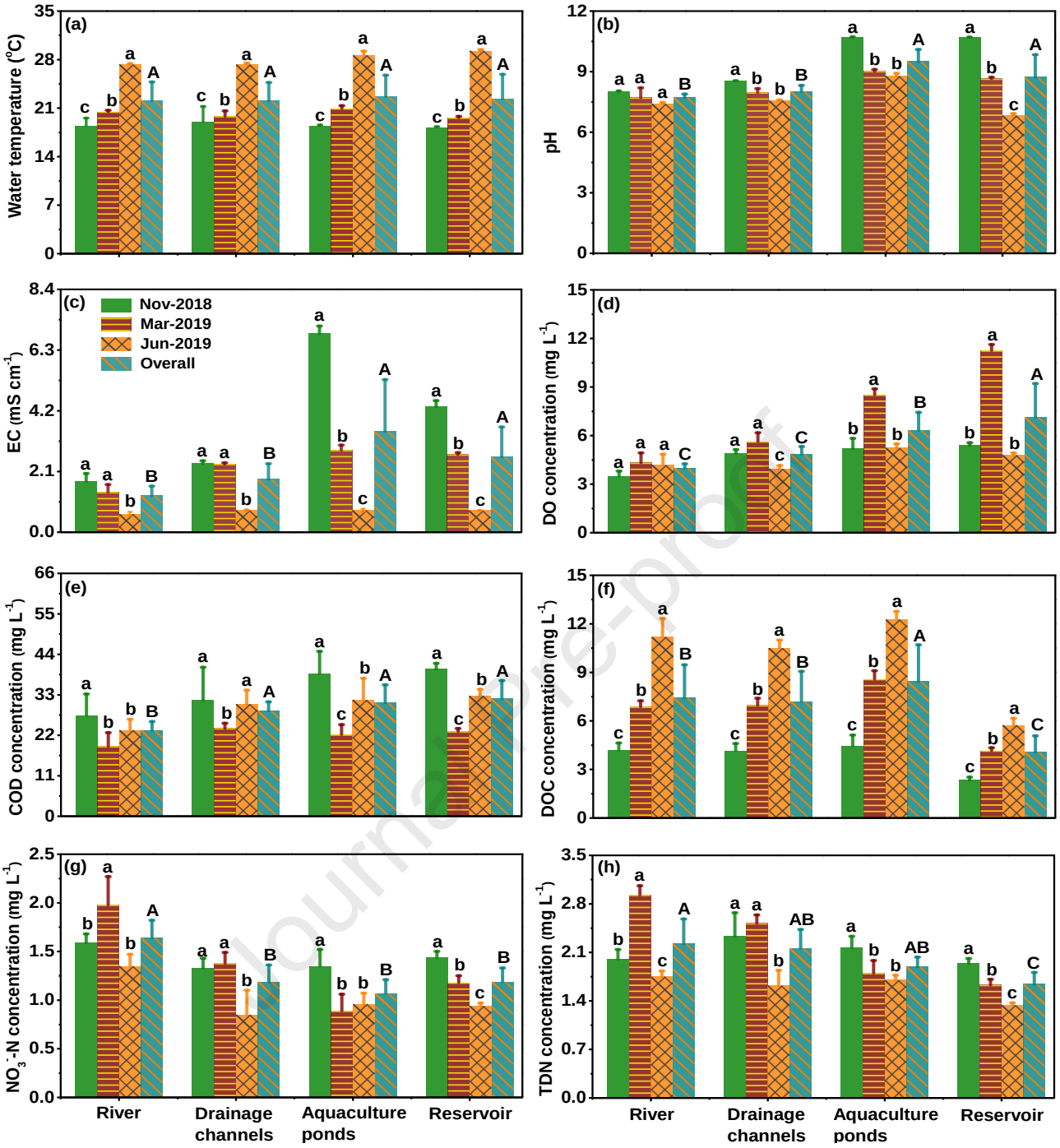

Fig. 2. Variations in (a) water temperature (T_w), (b) pH, (c) conductivity (EC), (d) dissolved oxygen (DO), (e) chemical oxygen demand (COD), (f) dissolved organic carbon (DOC), (g) NO_3^--N and (h) total dissolved nitrogen (TDN) in surface water (~0.2 m depth) among different sampling water bodies (river, drainage channels, aquaculture pond and reservoir) during each sampling campaign. Different lowercase letters above the bars indicate significant differences between months for specific sampling area (p<0.05). Different uppercase letters above the bars indicate significant differences between sampling areas (p<0.05). Differences in hydrographical properties between water bodies were tested by one-way analysis of variance (ANOVA). Bars represent mean ± SE.

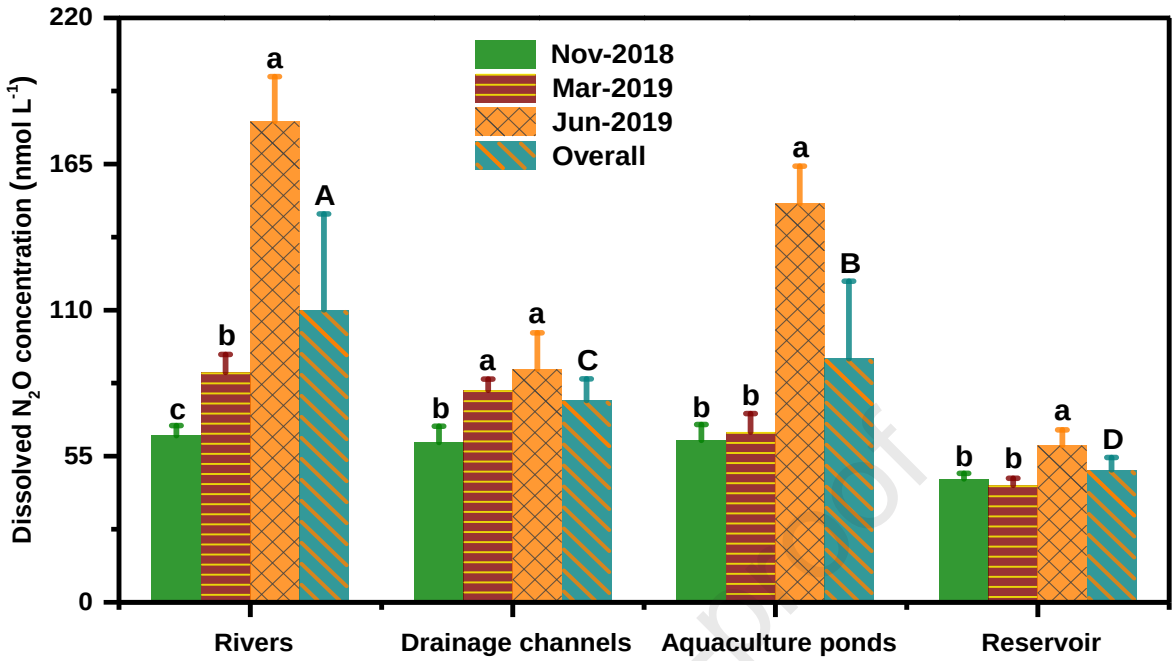

Fig. 3. Dissolved N_2O concentrations in surface water (~0.2 m depth) among different sampling water bodies (river, drainage channels, aquaculture ponds and reservoir) during each sampling campaign. Different lowercase letters above the bars indicate significant differences between months for specific sampling area (p<0.05). Different uppercase letters above the bars indicate significant differences between sampling areas (p<0.05). Bars represent mean ± SE.

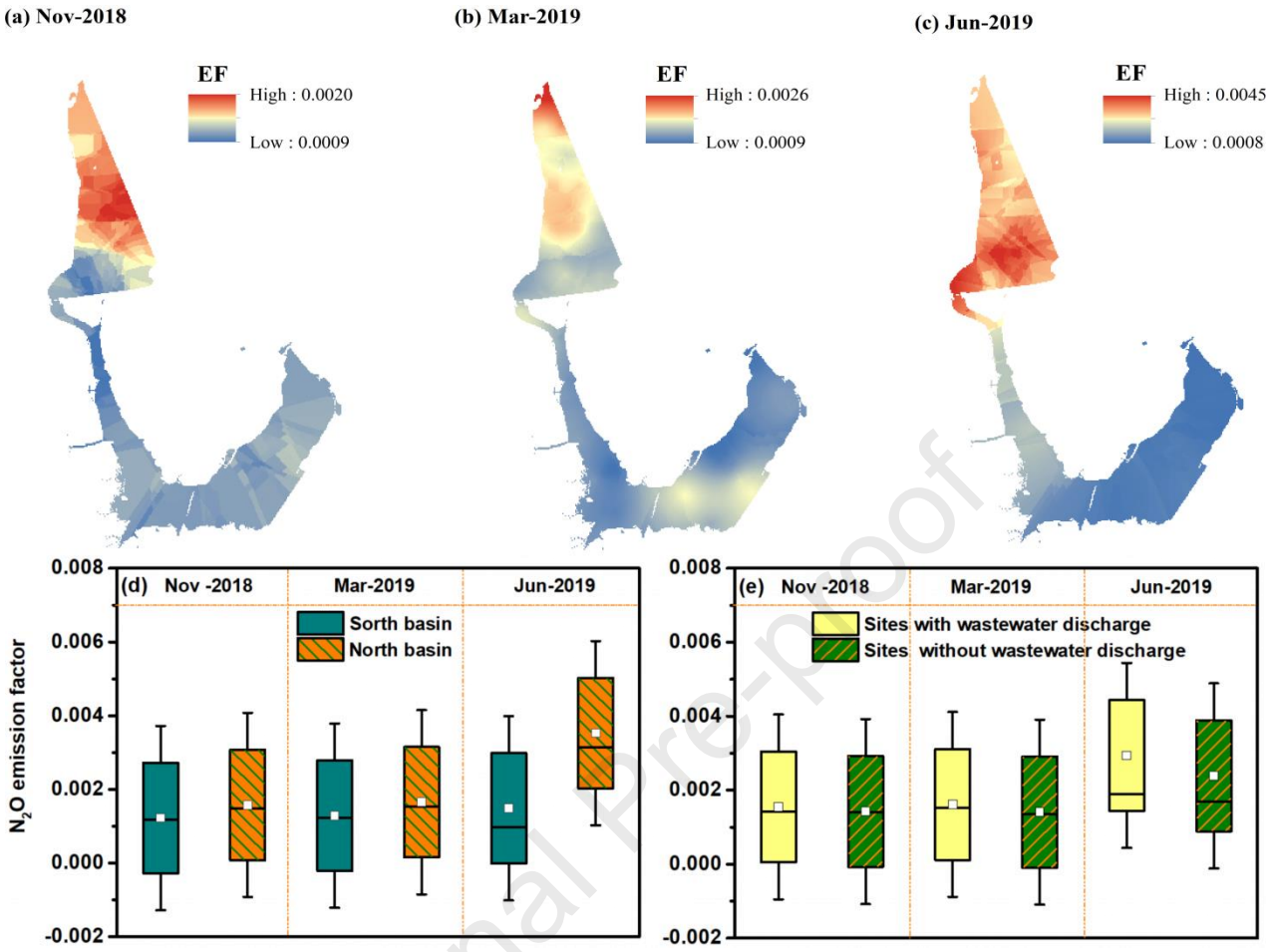

Fig. 4. Spatial distributions of N_2O emission factor (EF) in the Wenwusha Reservoir during each sampling campaign (a-c), Boxplots of N_2O emission factors at the (d) different reservoir basins (south basin (n = 47) *vs* north basin (n = 56)), and (e) sampling sites with wastewater discharge (n = 39) or without wastewater discharge (n = 64). Each box shows the quartiles and median, while the square and whiskers represent the mean and values within 1.5 times of the interquartile range, respectively.

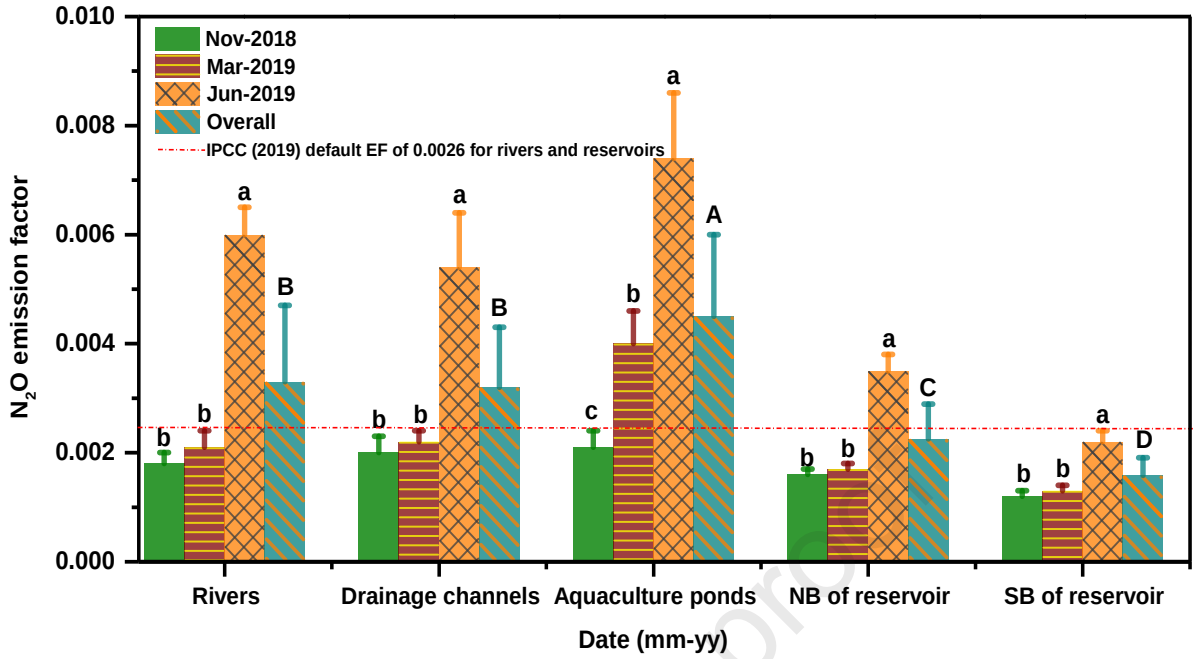

Fig. 5. N_2O emission factor (EF) among different sampling water bodies (river, drainage channels, aquaculture ponds and reservoir) during each sampling campaign. Different lowercase letters above the bars indicate significant differences between months for specific sampling area (p<0.05). Different uppercase letters above the bars indicate significant differences between sampling areas (p<0.05). Bars represent mean ± SE.

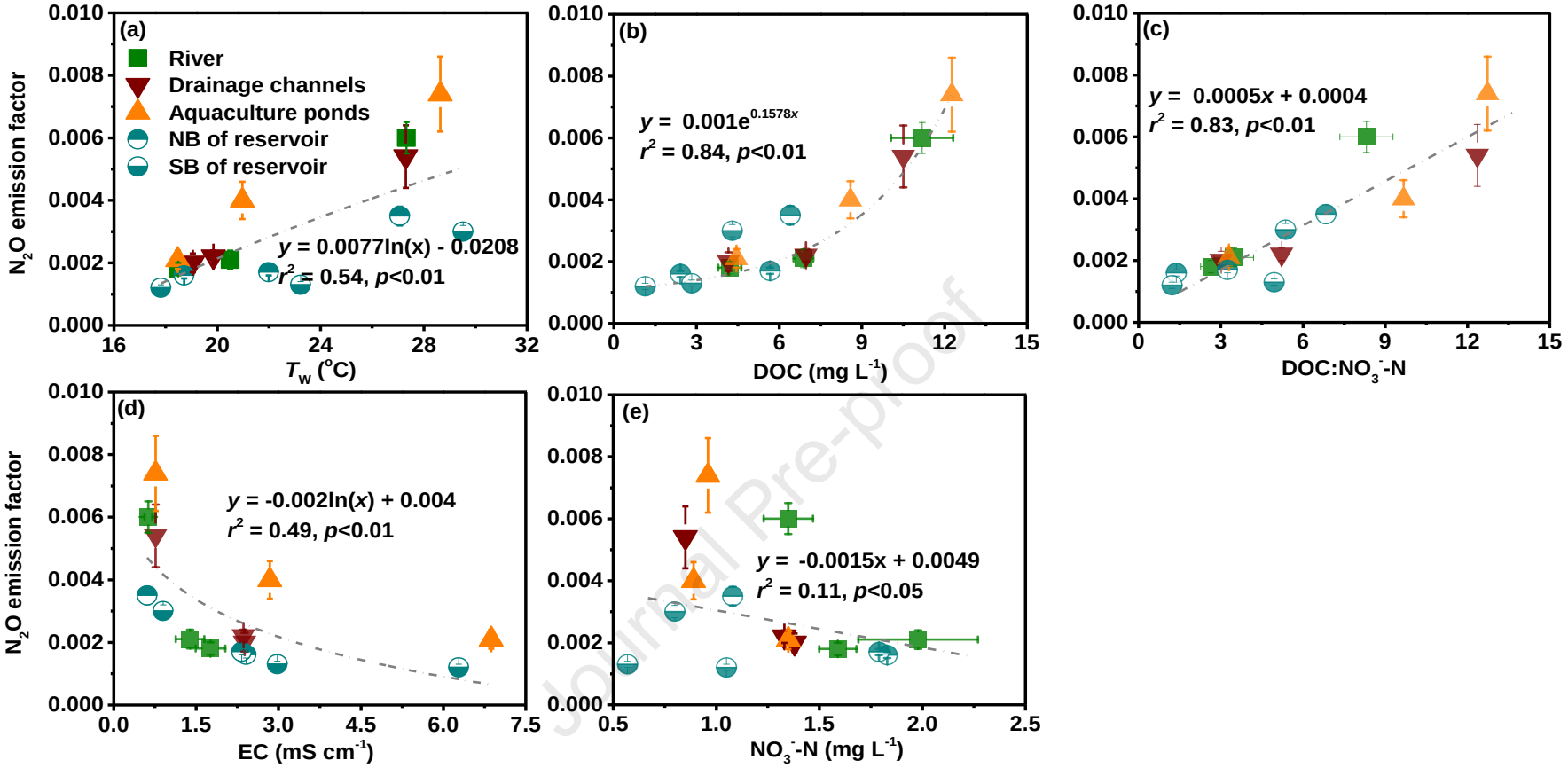

Fig. 6. Relationships between N_2O emission factor (EF) and (a) T_W, (b) DOC, (c) DOC:NO_3^--N, (e) EC and (d) NO_3^--N across all sampling water bodies (reservoir, river, drainage channels and aquaculture ponds) during the study period.

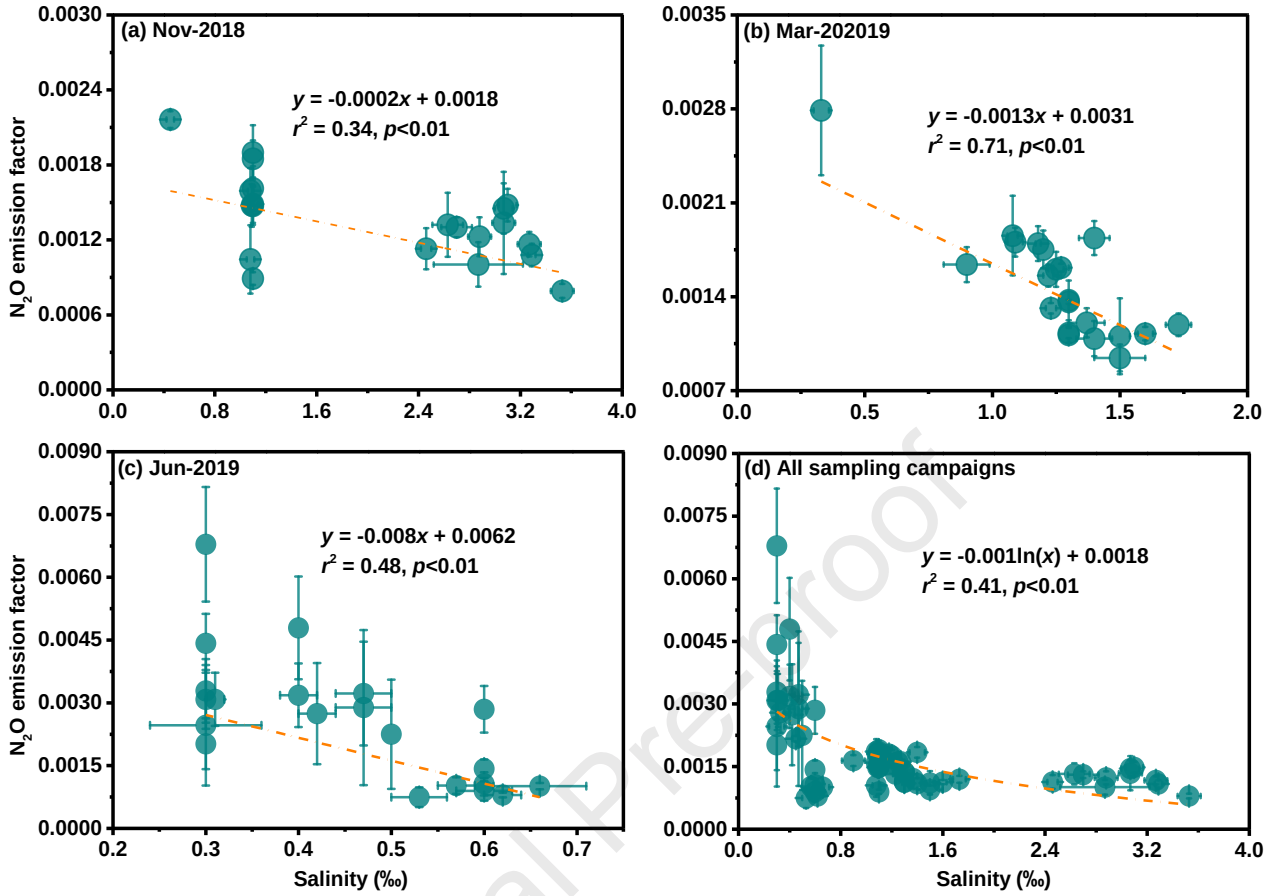

Fig. 7. Relationships between N_2O emission factor (EF) and surface-water salinity across 21 transects within the Wenwusha Reservoir during the Nov-2018 (a), Mar-2019 (b), Jun-2019 (c), and all sampling campaigns (d).

HIGHLIGHTS

- Coastal reservoirs are a strong source of nitrous oxide (N_2O)
- N_2O emission factor (EF) varied widely across different water types
- Water temperature (T_w) affected seasonal variations in EF
- Assessment of N_2O emissions using a fixed EF would introduce large errors
- EF was best predicted by T_w, dissolved organic carbon and nitrate concentration

Declaration of interests

☒The authors declare that they have no known competing financial interests or personal relationships that could have appeared to influence the work reported in this paper.

☐The authors declare the following financial interests/personal relationships which may be considered as potential competing interests: